16th World Conference on Earthquake, 16WCEE 2017

Santiago Chile, January 9th to 13th 2017

Paper N° 780 (Abstract ID)

Registration Code: S-S1464656324

SEISMIC RESPONSE OF CABLE-STAYED BRIDGES INDUCED BY GROUND MOTIONS WITH DIFFERENT SITES RELATIVE TO FAULT RUPTURE

S. Li (1), F. Zhang (2), J.Q. Wang(3)

(1) Ph.D. Candidate, Key Laboratory of Concrete and Prestressed Concrete Structure of China Ministry of Education, Southeast University, Nanjing 210096, China. E-mail: reallyreallyfan@vip.qq.com

(2) Ph.D. Candidate, Key Laboratory of Concrete and Prestressed Concrete Structure of China Ministry of Education, Southeast University, Nanjing 210096, China. E-mail: hmlishuai@163.com

(3) Associate Professor, Key Laboratory of Concrete and Prestressed Concrete Structure of China Ministry of Education, Southeast University, Nanjing 210096, China. (corresponding author). E-mail: wangjignquan@seu.edu.cn

Abstract

The focus of this paper is to determine the seismic response of a cable-stayed bridge subjected to near-fault ground motions in different fault regions considering soil-structure interaction (SSI) effects. Based on the sites relative to the fault rupture, the spatial positions of the records are divided into three regions, named Forward Region (FR), Middle Region (MR) and Backward Region (BR). Three groups of near-fault ground motions in above regions are selected as the input from the 1999 Chi-Chi earthquake. The Sutong Cable-stayed Bridge (SCB), with a main span of 1088 m, is taken as an example. The results reveal that the properties of near-fault ground motions have obvious correlations with the dynamic responses of the bridge in 3 regions. The PGV and PGA can be identified as the key parameters governing the bridge response in MR. The intensity measure parameter of near-fault ground motions in FR suitable for the super-span bridge systems can be taken as PGV and PGV/PGA. For the bridges located in BR, the PGA, and fault distance can be preferentially selected as the governing parameter in BR.

Keywords: near-fault ground motions, soil-structure interaction, cable-stayed bridge, rupture spatial position, fault region

1. Introduction

Sites located in proximity to active fault systems are prone to phenomena collectively known as near fault seismic effects, which is significantly different from those at far-fault region. The distinct characteristics of near-fault ground motions are derived from the rupture forward directivity, fling-step effect, hanging wall effect, etc. [1-3]. Researchers pay more attentions on structural response to near-fault ground motions in recent years [4-6]. The near-fault ground motions are strongly influenced by the faulting mechanism and the location of the recording station relative to the fault [3]. The spatial positions of the recording stations play an important role on the characteristics of near-fault records. Based on the site position along the fault, three regions are divided in the paper, called Forward Region (FR), Middle Region (MR) and Backward Region (BR) as shown in Fig. 1. In Fig. 1 three design scenarios are considered to evaluate the impact of near fault conditions on the performance of structures. A large effort has been made on the effect of pulse-type motions recorded at MR on the seismic response of structures in the near-fault zone [7-10]. However, these studies did not incorporate the effects of site regions on the performance of structures. Considering the spatial variations in the amplitude and duration of near-fault records in different regions, structures may have different seismic demand. Hence, extensive research work in this area is necessary.

Besides, when a structure is subjected to strong near-fault ground motions, consideration of soil-structure interaction (SSI) would be critical to understand its seismic response. Numerous studies have shown that the dynamic response of a structure supported on a flexible soil may differ significantly from that of the same structure with a rigid base [11-14]. SSI effects elongate the fundamental period of the structure as a result of the system's stiffness reduction. Hence, the common conception of SSI effects is their beneficial role on structural response. However, considering the long-period characteristics of near-fault ground motions [e.g. the period of TCU053 (CHI-CHI earthquake, 1999) exceeds 13s], SSI effects may be detrimental for long-period structures. While considering long-period life-line structures, especially long-span bridges, it is essential to fully understand the significance of near-fault effects and SSI effects. In this regard, it would be necessary to study the near-fault effects on the responses of long-period structures including SSI.

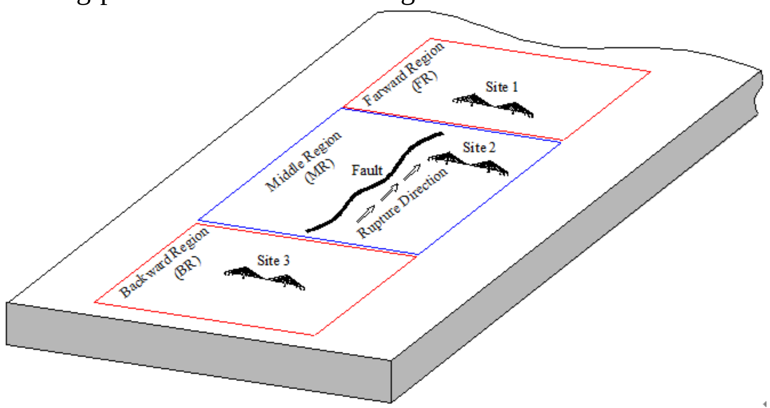

Fig. 1 – Schematic representation of site-source configuration

The intensity measure parameters of ground motions (e.g. PGV, PGA, PGV/PGA and so on) are a bridge linking the seismic analysis with structural demand parameters. It is essential to find the optimal intensity measure parameters of near-fault ground motions which can be used to govern the structural response in a certain fault region. It will be then helpful for the practicing engineers for the seismic design of such bridges. Ground motion selection provides the necessary link between seismic hazard and structural response [15, 16]. The ground motion uncertainty contributes significantly to uncertainty in structural analysis output. To select representative ground motions and effectively assess the performance of a structure at a given location, the relationship between the intensity measure parameters of near-fault ground motion and the dynamic response characteristics of structures have been investigated in previous studies [17-19]. Due to the distinct characteristics of near-fault ground motions, the ground motion intensity is difficult to be characterized by single index. Hence, the correlation analysis between intensity parameters and demand parameters needs to be implemented as an effective and systematic approach.

The focus of this paper is to determine the effects of near-fault ground motions (recorded by stations located in different fault regions) on the seismic response of long-period bridge structures including SSI effects. Based on the sites relative to the fault rupture, the spatial positions are divided into three regions, named Forward Region (FR), Middle Region (MR) and Backward Region (BR). To avoid the interference of different source mechanism, three sets of near-fault ground motions in the above regions are selected as the input from the 1999 Taiwan Chi-Chi earthquake. Taking the Sutong Cable-stayed Bridge (SCB) as a case study, the earthquake behavior of the bridge including SSI is compared under near-fault ground motions recorded at the above regions. Six commonly used indices are taken as intensity measure candidates of near-fault ground motions. Meanwhile, the horizontal displacement at top of the tower, the shear force and bending moment at the base of the tower are chosen as the response parameters. The correlation analysis between the intensity measure parameters and the response parameters is performed.

2. Near-fault ground motions

34 fault-normal near-fault ground motions in the three fault regions are selected as the input from the 1999 Taiwan Chi-Chi earthquake. The record stations are shown in Fig. 2.

The near-fault records are taken from the latest database of the PEER Next Generation Attenuation phase 2 (PEER NGA-West 2). Table 1 lists the basic properties of the ground motions such as the closest distance to fault rupture R_{rup}, site condition *S*, PGA (peak ground acceleration), PGV, PGD and PGV/PGA. The large ratios of PGV/PGA of ground motions imply that these records could contain velocity pulses, and for the non-pulse ground motions the ratios are usually smaller than 0.20. In order to avoid the interference to the nature of near-fault ground motions, these original records are employed and no scaling is performed in the response spectra and seismic analysis in the next sections.

Table 1 – Parameters of near-fault ground motions with different spatial positions

Station	Station	R_{rup}	S	PGA	PGV	PGD	PGV/PGA
FR	TCU-015EW	49.81	C	105.11	48.47	61.25	0.46
	TCU-029EW	28.04	C	154.26	39.69	53.78	0.26
	TCU-031EW	30.17	D	105.00	57.82	67.47	0.55
	TCU-033EW	40.88	C	145.96	46.15	53.69	0.32
	TCU-034E	35.68	C	241.20	44.51	46.74	0.18
	TCU-036EW	19.83	D	130.98	74.20	48.83	0.57
	TCU-039EW	19.89	C	195.87	64.72	72.10	0.33
	TCU-046EW	16.74	C	124.85	37.29	44.57	0.30
	TCU-087EW	6.98	C	124.15	39.97	56.90	0.32
	TCU-098EW	47.67	D	85.89	48.06	54.13	0.56
	TCU-128EW	13.13	C	129.05	73.97	91.54	0.57
MR	TCU-052EW	1.84	D	348.6	183.2	188.53	0.53
	TCU-065EW	2.49	D	773.3	132.4	93.23	0.17
	TCU-067EW	1.11	D	488.6	97.4	98.32	0.2
	TCU-074EW	13.75	D	585.9	70.22	208.45	0.12
	TCU-075EW	3.38	D	325.4	116.2	171.07	0.36
	TCU-079EW	10.95	D	577.4	67.49	14.91	0.12
	TCU-084EW	11.4	C	989.2	116.3	38.16	0.12
	TCU-101EW	2.9	C	200.0	67.9	71.94	0.34
	TCU-102EW	1.8	C	300.0	112.4	87.74	0.37
	TCU-103EW	4.0	C	130.0	61.9	85.39	0.48
	TCU-120EW	9.87	C	223.0	62.61	54.16	0.28
	TCU-129EW	2.21	D	983.0	67.98	127.0	0.07
BR	CHY-006E	9.76	C	355.05	61.42	23.97	0.17
	CHY-010EW	19.96	C	189.58	23.84	9.34	0.13
	CHY-014EW	34.18	D	231.38	27.38	11.56	0.12
	CHY-028EW	3.12	C	674.35	72.89	16.71	0.11
	CHY-029EW	10.96	C	254.89	25.83	11.36	0.10
	CHY-035EW	12.65	C	255.59	48.89	10.65	0.19
	CHY-046EW	24.1	C	140.00	23.24	10.35	0.17
	CHY-047EW	24.13	E	155.00	23.46	20.72	0.15
	CHY-074EW	10.8	C	228.06	35.82	17.00	0.16
	CHY-087EW	28.91	C	139.17	11.61	5.85	0.08
	CHY-088EW	37.48	D	131.75	19.20	7.59	0.15

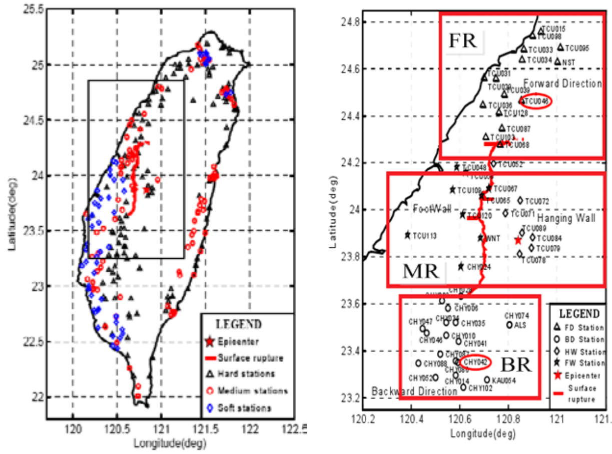

Fig. 2 – Stations distribution of Chi-Chi (Taiwan) earthquake

3. Response spectra of ground motions

In order to evaluate the characteristics of near-fault records with different spatial positions, the 5% damped elastic pseudo-acceleration and pseudo-velocity spectra of ground motions given in Table 1 are computed and the mean of the records in each ground motion category reasonably represent the response spectrum. The response spectra of the ground motions recorded at different regions are presented in Fig. 3.

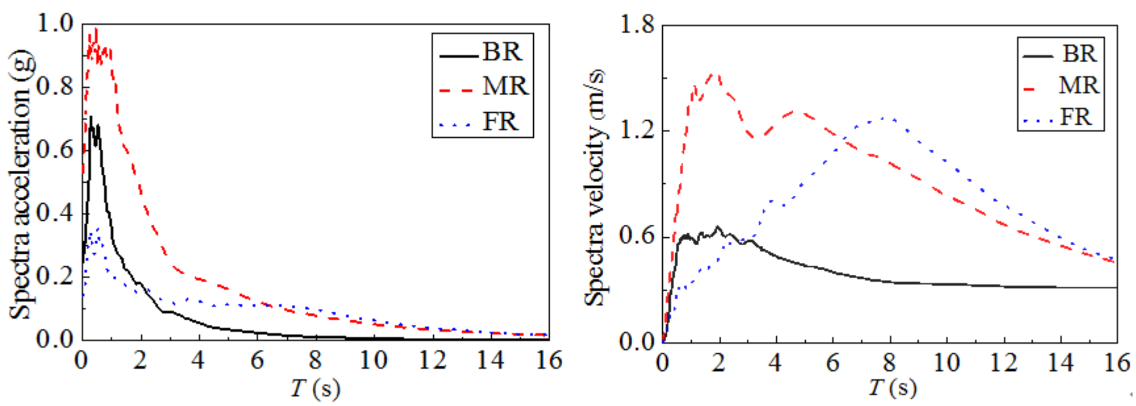

Fig. 3 – Response spectra of original near-fault ground motions with spatial position (a) pseudo-acceleration spectra (b) pseudo-velocity spectra

It can be observed in Fig. 3(a) that in the period region T=0-2.2 s, the spectra acceleration of the ground motions recorded in MR is much larger than that recorded in FR and BR. The spectral acceleration of these three types of near-fault ground motions attains the maximum at the vicinity of period 0.5s. For the long-period region T=2.2-16 s, the acceleration response spectra of the records in MR and FR shows obvious long-period portion, whereas that of the records in BR is much smaller. The phenomenon can be easily understood that some records in MR and FR exhibit a large velocity pulse. When the period exceeds 6.4s, the acceleration response of records in FR is almost the same as that in MR.

The elastic pseudo-velocity spectra are shown in Fig. 3(b). It can be seen that in the period region T=0-3.4 s, the records in MR have larger spectra velocity than that in FR and BR, and the mean value of the records in FR is the smallest. In the period region T=3.4-16 s, due to the impact of forward directivity effects, the spectra velocity of records in FR exhibits increasing trend and is greater than that in BR. When the period exceeds 6.4 s, the spectra velocity of records in FR is a little greater than that in MR.

4. Case study description

The bridge model used in this paper is the Sutong Cable-stayed Bridge (SCB) connecting Suzhou and Nantong City, China, which is the second-longest cable-stayed bridge in the world, with a main span of 1088 m (Fig. 4). The bridge has two approximately 300.4m inverted-Y pylons. The deck is a streamlined flat steel box girder having a width of 41.0m. There are 272 cable members, which are arranged in a fan configuration. Two auxiliary piers are constructed in each side span. The counterweights in the two side spans are applied to balance the weight of the main span. The configuration of the bridge is presented schematically in Fig. 5.

A 3D finite element (FE) model of the SCB is constructed to represent the full bridge system. The model relies on the commercial software ANSYS. The steel girders, transverse diaphragms, towers, and piers are modeled as elastic beam elements (Beam 4 in ANSYS). The girder is discretized based on the suspended points of the stayed cables. The cable stays are modeled as 3D tension-only truss elements (Link 10), and the nonlinear behavior of the inclined cable stays are idealized using the Ernst equation of equivalent modulus of elasticity. The translational degrees of transverse diaphragms and piers are coupled in the vertical and transverse directions. The three dimensional model is developed using 1883 joints and 2661 elements.

To explicitly investigate the effects of near-fault ground motions with different spatial positions on the performance of Sutong bridge, three design scenarios are considered in this paper that the bridge are supposed to be constructed in the FD, MD and BD, respectively (Fig. 1), and the longitudinal direction of the bridge perpendiculars to the fault. The selected ground motion records are applied in the longitudinal direction. The fault is shown in Fig. 5 and the parameter R_{jb} denotes the Joyner-Boore distance.

The pylon foundation system of Sutong Bridge is shown in Fig. 6. In order to investigate the influence of SSI effect on the responses of the bridge, systematic lumped-parameter models proposed by Wu and his co-workers [20] are used to simulate the soil-structure interaction effect in this study, as shown in Fig. 7. Note that the sum of the static stiffness of the individual piles presented by Budhu and Davies [21] is adopted to represent the stiffness of group piles. According to the modal analysis, SSI effects can elongate the period of the structure as a result of the system's stiffness reduction and affect the bridge response through a substantial change in nature of dominant shapes especially for the higher modes of vibrations compared to the bridge without SSI effect.

Fig. 4 – Sutong cable-stayed bridge

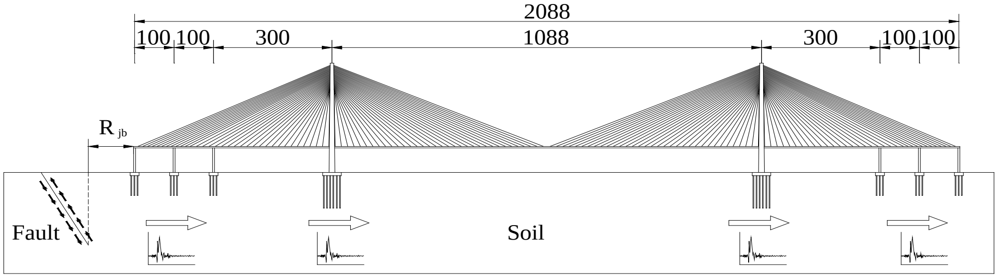

Fig. 5 – Elevation configuration of the SCB (meters)

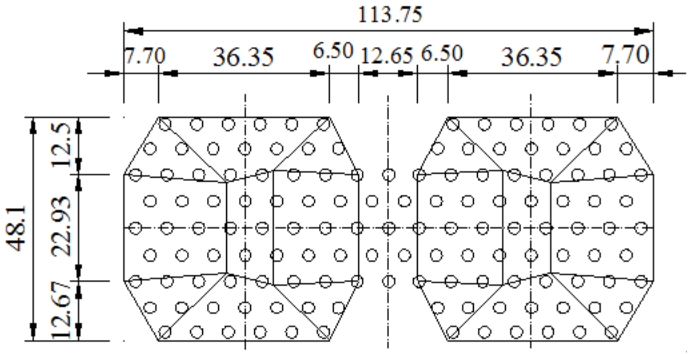

Fig. 6 – The foundation of the tower of the SCB (meters)

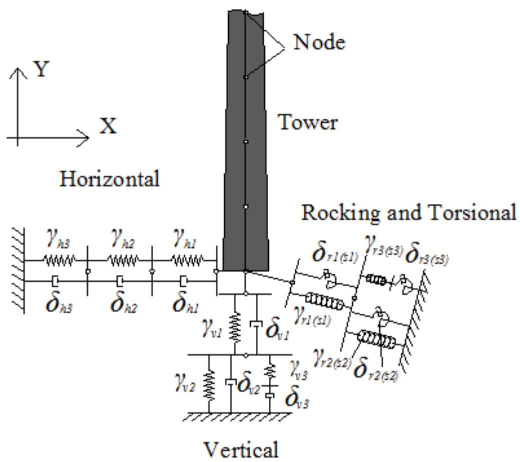

Fig. 7 – Discrete element model of structure -soil system in longitudinal direction

5. Correlation analyses between intensity parameters and response parameters of SCB

For the sake of simplification, six simple indices are taken as intensity measure candidates of near-fault ground motions, including input energy, PGV, PGA, PGD, PGV/PGA and fault distance. Meanwhile, based on the deformation and mechanical characteristics of the tower, the horizontal displacement at top of the tower, the shear force and bending moment at the base of the tower are chosen as the response parameters. The relationships between the intensity measure indices of near-fault ground motions and the response parameters are taken as examples and shown in Fig. 8-11. Table 2 shows the correlation coefficients of the seismic responses versus the intensity parameters.

According to the correlation coefficient, the degree of the correlation can be divided into three levels, namely the low-correlation (0~0.3), the high-correlation (0.3~0.6), and the remarkable-correlation (0.6~1). From the Figures and Table 3, the detailed observation is given as follows.

1. Due to the variability of the ground motions in different fault regions, the response parameters show very different correlation with the intensity parameters. For the three design scenarios, the parameter PGV shows very good relation with the response parameters. Obviously, using the most commonly applied parameter PGA in earthquake engineering as the key intensity indices is unreasonable for the structures located in the near-fault zone.

2. For the bridge located in FR, the intensity indices with very good correlation are PGV and PGV/PGA. The PGD and input energy show high correlation with the response parameters, and the coefficients range from 0.391 to 0.545. Whereas, the PGA and fault distance do not correlate well with the response parameters. This phenomenon is attributed to the abundant low-frequency components of impulsive ground motions in FR. As

can be seen in Table1, the values of impulsive parameter PGV/PGA of the records in FR range from 0.18 to 0.57 and are higher than those of records in MR and BR. Hence, for the seismic design of the bridges located in FR, the PGV and PGV/PGA can be utilized to reasonably assess the bridge responses in FR.

3. For the bridge located in MR, the input energy and PGV are fairly correlated with the displacement of the tower. Considering the abundant low-frequency components of impulsive ground motions in MR, the correlation coefficient of PGV with the displacement is larger than that of input energy, and the coefficient is 0.79. Hence, PGV can be used to evaluate the displacement response of the bridge in this region. The index PGV and PGA correlates well with the the internal force of the tower, and the correlation coefficients range from 0.497 to 0.832. Based on the analysis, the PGV and PGA can be identified as the key parameters governing the bridge response in MR.

4. For the bridge located in BR, the response parameters with very good correlation are PGD, PGV, PGA and fault distance, and the correlation coefficients ranges from 0.527 to 0.964. The input energy shows strong correlation with the displacement response, and the coefficient is 0.855. Because the records in this region show non-impulsive characteristic, the impulsive parameter PGV/PGA do not correlate well with the response parameters. It should be noted that fault distance has an obvious influence on the attenuation of the records in the region. The correlation coefficients between the fault distance and the response parameters are negative, and the coefficients range from -0.636 to -0.745. Therefore, the PGA, PGV, PGD and fault distance can be selected as the governing parameter in BR. For the sake of simplification in the structural seismic design, the fault distance and PGA can be preferentially identified as the key parameters in BR.

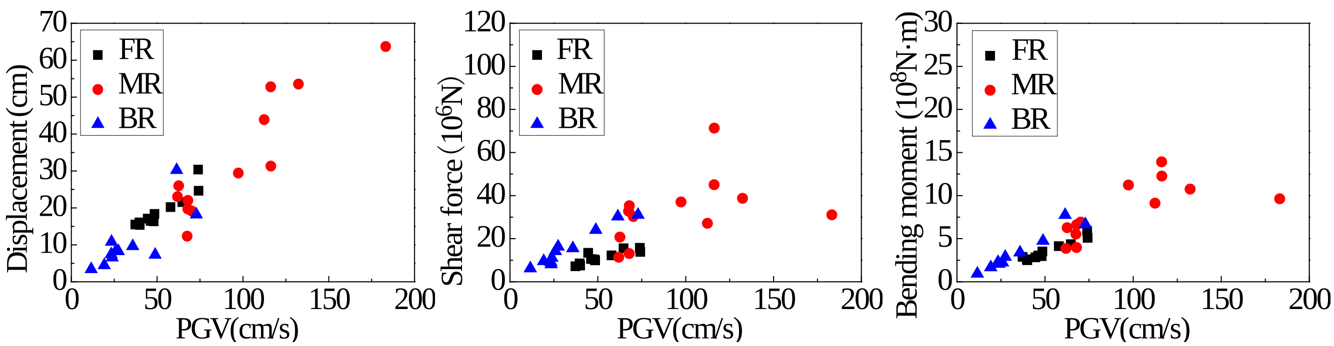

(a) (b) (c)

Fig. 8 – Influence of PGV on seismic responses of cable-stayed bridge (a) the longitudinal displacement at the top of the tower (b) the shear force at the base of the tower (c) the bending moment at the base of the tower

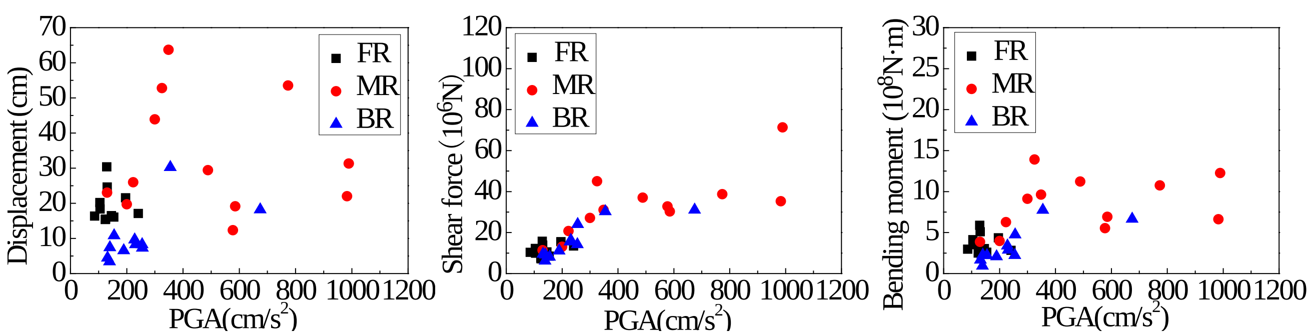

(a) (b) (c)

Fig. 9 – Influence of PGA on seismic responses of cable-stayed bridge (a) the longitudinal displacement at the top of the tower (b) the shear force at the base of the tower (c) the bending moment at the base of the tower

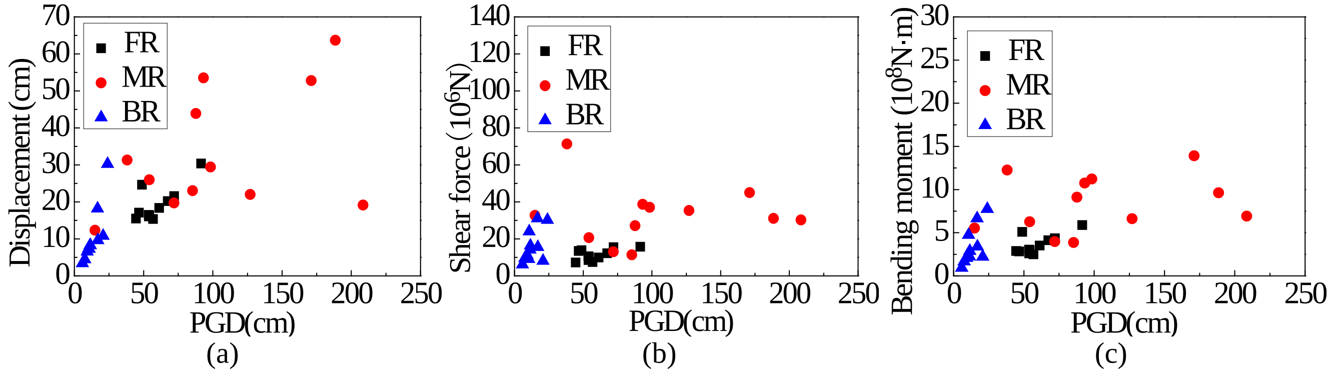

Fig. 10 – Influence of PGD on seismic responses of cable-stayed bridge (a) the longitudinal displacement at the top of the tower (b) the shear force at the base of the tower (c) the bending moment at the base of the tower

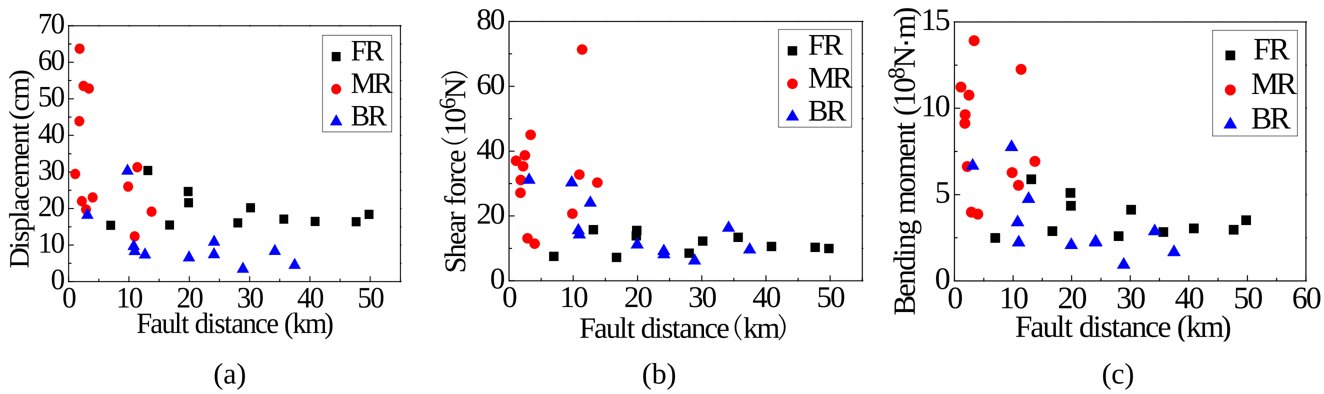

Fig. 11 – Influence of fault distance on seismic responses of cable-stayed bridge (a) the longitudinal displacement at the top of the tower (b) the shear force at the base of the tower (c) the bending moment at the base of the tower

Table 2 – Correlation coefficients between intensity indices of ground motions and response parameters of SCB

Intensity indices	**FR**			**MR**			**BR**		
	D	**F**	**M**	**D**	**F**	**M**	**D**	**F**	**M**
Input energy	0.545	0.391	0.436	0.741	0.091	0.203	0.855	0.400	0.527
PGA	0.164	0.364	-0.045	0.035	0.769	0.497	0.682	0.909	0.864
PGV	0.927	0.836	0.903	0.790	0.664	0.832	0.672	0.955	0.936
PGD	0.482	0.427	0.491	0.308	0.140	0.371	0.964	0.527	0.718
PGV/PGA	0.662	0.511	0.795	0.507	-0.451	-0.056	0.196	0.224	0.470
Fault distance	0.245	0.210	-0.042	-0.497	-0.028	-0.217	-0.636	-0.682	-0.745

Note: D denotes the longitudinal displacement at the top of the tower; F denotes the shear force at the base of the tower; M denotes the bending moment at the base of the tower.

6. Conclusions

The seismic responses of the Sutong cable-stayed bridge (SCB) including SSI effects subjected to near-fault ground motions in three different fault regions, including the Forward Region (FR), Middle Region (MR) and Backward Region (BR), are examined in this paper. A total of 46 near-fault ground motions from the 1999 Taiwan Chi-Chi earthquake are selected as seismic input containing the records in FR (11 records), MR (12 fault-normal records and 12 fault-parallel records) and BR (11 records). The earthquake behavior of the bridge including SSI is assessed under near-fault ground motions recorded at the above regions. The correlation coefficients between 6 commonly used intensity indices and 3 response parameters of the SCB are computed. Through the numerical analysis and comparison, some concluding remarks are drawn below.

1. The ground motions in Middle Region and Forward Region have abundant low-frequency components, whereas the high-frequency components of the ground motions in Backward Region are generally significant. The spectral acceleration and velocity values of fault-normal ground motions are greater than those of fault-parallel ground motions.

2. SSI effects elongate the period of the structure as a result of the system's stiffness reduction and affect the bridge response through a substantial change in nature of dominant shapes especially for the higher modes of vibrations. Inclusion of SSI is essential for effective design of the super-span cable-stayed bridge systems.

3. The intensity measure parameter of near-fault ground motions in FR suitable for the super-span bridge systems can be taken as PGV and PGV/PGA. For the bridge systems located in MR, PGV and PGA are the intensity index of the near-fault ground motions. For the bridges located in BR, all the PGA, PGV, PGD and fault distance can be selected as the governing parameter in BR. For the sake of simplification in the structural seismic design, the fault distance and PGA can be preferentially identified as the key parameters in BR.

Finally, it should be noted that the above observation and conclusion are strictly valid for the super-span long-period bridge systems located in different fault regions, and need to be updated for the short-period and medium-period bridge systems considering the difference of the fundamental period.

7. Acknowledgements

This study was supported by National Natural Science Foundation of China (Grant No. 51378110 and 51528802), Graduate Student Research Innovation Project of Jiangsu Province (Grant No. KYLX15_0086) and Priority Academic Program Development of Jiangsu Higher Education Institutions (Grant No. CE02-2-6). The financial supports are greatly appreciated.

8. Copyrights

9. References

[1] Bertero VV, Mahin SA, Herrea RA (1978): A seismic design implications of near-fault San Fernando and structure dynamic. Earthquake Engineering and Structural Dynamics, 6(1): 31-42.

[2] Mavroeidis GP, Dong G, Papageorgiou AS (2004): Near-fault ground motions, and the response of elastic and inelastic single-degree-of-freedom (SDOF) systems. Earthquake Engineering and Structural Dynamics, 33(9): 1023-1049.

[3] Somerville PG, Smith NF, Graves RW, Abrahamson NA (1997): Modification of empirical strong ground motion attenuation relations to include the amplitude and duration effects of rupture directivity. Seismological Research Letters, 68(1):199-222.

[4] Baltzopoulos G, Chioccarelli E, Iervolino I (2015): The displacement coefficient method in near-source conditions. Earthquake Engineering and Structural Dynamics, 44(7): 1015-1033.

[5] Bray JD, Rodriguez MA (2004): Characterization of forward-directivity ground motions in the near-fault region. Soil Dynamics and Earthquake Engineering, 24(5):815-828.

[6] Zhang S, Wang G (2013): Effects of near-fault and far-fault ground motions on nonlinear dynamic response and seismic damage of concrete gravity dams. Soil Dynamics and Earthquake Engineering, 53: 217-229.

[7] Kalkan E, Kunnath SK (2006): Effects of fling step and forward directivity on seismic response of buildings. Earthquake Spectra, 22(2): 367-390.

[8] Saiidi MS, Vosooghi A, Choi H, Somerville P (2014): Shake table studies and analysis of a two-span RC bridge model subjected to a fault rupture. Journal of Bridge Engineering, , 19, DOI: 10.1061/(ASCE)BE.1943-5592.0000478.

[9] Yang D, Pan J, Li G (2010): Interstory drift ratio of building structures subjected to near-fault ground motions based on generalized drift spectral analysis. Soil Dynamics and Earthquake Engineering, 30(11): 1182-1197.

[10] Wu G, Zhai C, Li S (2014): Effects of near-fault ground motions and equivalent pulses on Large Crossing Transmission Tower-line System. Engineering Structures, 77: 161-169.

[11] Spyrakos CC (1990): Assessment of SSI on the longitudinal seismic response of short span bridges. Engineering Structures, 12(1): 60-66.

[12] Zhang J, Tang Y (2009): Dimensional analysis of structures with translating and rocking foundations under near-fault ground motions. Soil dynamics and earthquake engineering, 29(10): 1330-1346.

[13] Masaeli H, Khoshnoudian F, Ziaei R (2015): Rocking soil-structure systems subjected to near-fault pulses. Journal of Earthquake Engineering, 19(3): 461-479.

[14] Khoshnoudian F, Ahmadi E (2013): Effects of pulse period of near‐field ground motions on the seismic demands of soil–MDOF structure systems using mathematical pulse models. Earthquake Engineering & Structural Dynamics, 42(11): 1565-1582.

[15] Lin T, Haselton CB, Baker JW (2013): Conditional spectrum-based ground motion selection. Part I: Hazard consistency for risk-based assessments. Earthquake engineering and structural dynamics, 42(12): 1847-1865.

[16] Lin T, Haselton CB, Baker JW (2013): Conditional Spectrum-Based Ground Motion Selection. Part II: Intensity-Based Assessments and Evaluation of Alternative Target Spectra. Earthquake Engineering and Structural Dynamics, 42: 1867-1884.

[17] Liao WI, Loh CH, Lee BH (2004): Comparison of dynamic response of isolated and non-isolated continuous girder bridges subjected to near-fault ground motions. Engineering Structures, 26: 2173-2183.

[18] Han M, Duan YL, Sun H, Sheng W (2013): Influence of characteristics parameters of near-fault ground motions on the seismic responses of base-isolated structures. China Civil Engineering Journal, 46(6): 8-13(in Chinese)

[19] Yang DX, Pan JW, Li G (2009): Non-structure-specific intensity measure parameters and characteristic period of near-fault ground motions. Earthquake Engineering and Structural Dynamics, 38: 1257-1280.

[20] Wu WH, Lee WH (2002): Systematic lumped-parameter models for foundations based on polynomial-fraction approximation. Earthquake engineering & structural dynamics, 31(7): 1383-1412.

[21] Davies TG, Budhu M, Davies TG (1986): Non-linear analysis of laterally loaded piles in heavily overconsolidated clays. Géotechnique, 36(4):527-538.